Modelling of high-power supercontinuum generation in highly nonlinear, dispersion shifted fibers at CW pump

Serguei M. Kobtsev and Serguei V. Smirnov
Novosibirsk State University, Pirogova 2, Novosibirsk 630090, Russia
kobtsev@lab.nsu.ru

Abstract: For the first time a remarkably exact match was achieved of the results from modelling of CW-pumped SC in a highly non-linear fibre with experiment (A.K. Abeeluck *et al*. Opt. Lett. **29**, 2163-2165 (2004)) where a wide-band SC in the 1200–1780-nm range was reported. Our simulation results show that decay of CW pump radiation into a train of sub-picosecond pulses induced by the modulation instability leads to formation of optical solitons. Energy and carrier frequency of the solitons are random parameters because of quantum noise in the pump radiation. We found that a relatively smooth SC spectrum obtained by us from modelling and observed experimentally comes from averaging of a large number of soliton spectra and the spectrum of short-wavelength non-soliton radiation that is generated because of resonant pumping of energy from solitons.

OCIS codes: (190.0190) Nonlinear optics; (190.4370) Nonlinear optics, fibers

References and links

1. J.K. Ranka, R.S. Windeler, and A.J. Stentz, "Visible continuum generation in air-silica microstructure optical fibers with anomalous dispersion at 800 nm," Opt. Lett. **25**, 25-27 (2000).
2. W. Drexler, U. Morgner, F.X. Kärtner, C. Pitris, S.A. Boppart, X.D. Li, E.P. Ippen, and J.G. Fujimoto, "In vivo ultrahigh-resolution optical coherence tomography," Opt. Lett. **24**, 1221-1224 (1999).
3. Y.M. Wang, Y.H. Zhao, J.S. Nelson, Z.P. Chen, and R.S. Windeler, "Ultrahigh-resolution optical coherence tomography by broadband continuum generation from a photonic crystal fiber," Opt. Lett. **28**, 182-184 (2003).
4. W. Drexler, "Ultrahigh-resolution optical coherence tomography," J. Biomed. Opt. **9**, 47-74 (2004).
5. D.A. Jones, S.A. Diddams, J.K. Ranka, A. Stentz, R.S. Windeler, J.L. Hall, and S.T. Cundiff, "Carrier-envelope phase control of femtosecond mode-locked lasers and direct optical frequency synthesis," Sc. **288**, 635-639 (2000).
6. R. Holzwarth, M. Zimmermann, Th. Udem, T.W. Hänsch, A. Nevsky, J. Von Zanthier, H. Walther, J.C. Knight, W.J. Wadsworth, P.St.J. Russell, M.N. Skvortsov, and S.N. Bagayev, "Absolute frequency measurement of iodine lines with a femtosecond optical synthesizer," Appl. Phys. B **73**, 269-271 (2001).
7. S.A. Diddams, D.J. Jones, J. Ye, S.T. Cundiff, J.L. Hall, J.K. Ranka, and R.S. Windeler, "Direct rf to optical frequency measurements with a femtosecond laser comb," IEEE Trans. Instrum. Meas. **50**, 552-555 (2001).
8. A.K. Abeeluck, C. Headley, and C.G. Jørgensen, "High-power supercontinuum generation in highly nonlinear, dispersion-shifted fibers by use of a continuous-wave Raman fiber laser," Opt. Lett. **29**, 2163-2165 (2004).
9. J.W. Nicholson, A.K. Abeeluck, C. Headley, M.F. Yan, and C.G. Jørgensen, "Pulsed and continuous-wave supercontinuum generation in highly nonlinear, dispersion-shifted fibers." Appl. Phys. B **77**, 211-218 (2003).
10. M. González-Herráez, S. Martín-López, P. Corredera, M.L. Hernanz, and P.R. Horche, "Supercontinuum generation using a continuous-wave Raman fiber laser," Opt. Comm. **226**, 323-328 (2003)
11. A.V. Avdokhin, S.V. Popov, and J.R. Taylor, "Continuous-wave, high-power, Raman continuum generation in holey fibers," Opt. Lett. **28**, 1353-1355 (2003).

#8055 - $15.00 USD Received 8 July 2005; revised 18 August 2005; accepted 22 August 2005

12. J.N. Kutz, C. Lyngå, and B.J. Eggleton, "Enhanced supercontinuum generation through dispersion-management," Opt. Express **13**, 3989-3998 (2005). http://www.opticsexpress.org/abstract.cfm?URI=OPEX-13-11-3989
13. A. Apolonski, B. Povazay, A. Unterhuber, W. Drexler, W.J. Wadsworth, J.C. Knight, and P.S.J. Russell, "Spectral shaping of supercontinuum in a cobweb photonic-crystal fiber with sub-20-fs pulses," J. Opt. Soc. Am. B **19**, 2165-2170 (2002).
14. J. Teipel, K. Franke, D. Turke, F. Warken, D. Meiser, M. Leuschner, and H. Giessen, "Characteristics of supercontinuum generation in tapered fibers using femtosecond laser pulses," Appl. Phys. B **77**, 245-251 (2003).
15. E.A. Golovchenko, P.V. Mamyshev, A.N. Pilipetskii, and E.M. Dianov, "Numerical analysis of the Raman spectrum evolution and soliton pulse generation in single-mode fibers," J. Opt. Soc. Am. B **8**, 1626-1632 (1991).
16. G.P. Agrawal, *Nonlinear Fiber Optics* (Academic Press, San Diego, California, 2001).
17. K.J. Blow and D. Wood, "Theoretical description of transient stimulated raman scattering in optical fibers," J. Quantum. Electron. **25**, 2665-2673 (1989).
18. J. Herrmann, U. Griebner, N. Zhavoronkov, A. Husakou, D. Nickel, J.C. Knight, W.J. Wadsworth, P.St.J. Russell and G. Korn, "Experimental evidence for supercontinuum generation by fission of higher-order solitons in photonic fibers," Phys. Rev. Lett. **88**, 173901 (2002)
19. M.N. Islam, G. Sucha, I. Bar-Joseph, M. Wegener, J.P. Gordon, and D.S. Chemla, "Femtosecond distributed soliton spectrum in fibers," J. Opt. Soc. Am. B **6**, 1149-1158 (1989).
20. T.J. Ellingham, J.D. Ania-Castañón, S.K. Turitsyn, A.A.Pustovskikh, S.M.Kobtsev, and M.P.Fedoruk. "Dual-pump Raman amplification with increased flatness using modulation instability," Opt. Express **13**, 1079-1084 (2005). http://www.opticsexpress.org/abstract.cfm?URI=OPEX-13-4-1079

1. Introduction

The effect of continuum (or supercontinuum (SC)) generation consists in significant broadening (up to two octaves or even more in the case of SC [1]) of pump radiation spectrum when this radiation propagates through a nonlinear medium. So far, wide continuum spectra have already been employed for development of multi-wavelength light sources used in telecommunications, allowed an improvement of longitudinal resolution in optical coherence tomography by more than an order of magnitude [2–4], facilitated a revolutionary break-through in optical frequency metrology [5–7], and found a number of other important applications.

Pulsed pump radiation is commonly used (mostly with the pulse duration in femto- and picosecond ranges), however recently a possibility of continuum generation (CG) with CW pump in the vicinity of the fibre zero-dispersion wavelength [8–11] was shown as well. Thus, for example, Abeeluck *et al.* with the use of pump from CW Raman fibre laser operated at 1486 nm and 0.5-km-long Highly Non-linear Fibre (HNLF) obtained a broad-band SC, covering the spectral range from 1200 nm up to 1780 nm.

Despite the fact that a large number of papers focused on simulation of CG with pulsed pump were published and that theoretical investigations of CG with CW pump have been already reported [12], the mechanisms of broad-band continuum generation are not completely understood both in the case of pulsed and in that of CW pump. Not only there is lack of deep familiarity with interplay of different non-linear optical effects responsible for generation of broad spectra, but there is also absence of quantitative agreement between numerical simulation and experiment. Moreover, in certain cases of CG with pulsed pump authors even point to qualitative discrepancy of theoretical predictions with experimental results [13,14].

In this paper we made an attempt to adequately simulate experimental results of SC generation in HNLF with the use of CW pump [8]. In prior publications [9,15] continuum generation in CW-pumped fibres was already studied with the help of numerical modelling based on the same equation that we use. However, these reports differ from ours in the method of CW pump modelling [9] and in modelling of noise [9,15]. Additionally, in the present report we applied for the first time the method of averaging spectra generated in a series of numerical experiments that included random noise in the pump. This gave us the

#8055 - $15.00 USD Received 8 July 2005; revised 18 August 2005; accepted 22 August 2005

opportunity to arrive at an excellent agreement between our calculations and the experiment [8] in a broad spectral domain, whereas the authors of Ref. [9] point out a substantial disagreement of the modeling results and the experimental data. In Ref. [15] no comparison with experiment was carried out.

To our knowledge this is the first article which reports a good qualitative and quantitative agreement between simulated and experimental continuum spectra for the maximum pump power level used in experiments. Physical mechanisms of spectral broadening are examined.

2. Numerical model

To simulate propagation of ultra-short laser pulses through optical fibres we use the generalized non-linear Schrödinger equation, which was derived without resorting to approximation of slowly varying amplitudes [16]:

$$\frac{\partial A}{\partial z} = i\sum_{k=2}^{k_{\max}} \frac{i^k}{k!}\beta_k \frac{\partial^k A}{\partial t^k} + i\gamma\left(1+\frac{i}{\omega_0}\frac{\partial}{\partial t}\right)\left(A(z,t)\int_0^{\infty} R(t')\left|A(z,t-t')\right|^2 dt'\right) \qquad (1)$$

where $A(z, t)$ – electric field envelope, β_k – dispersion coefficients at the pump frequency ω_0 and $\gamma = n_2\ \omega_0 / (A_{eff}\ c)$ – non-linear coefficient, where $n_2 = 3 \times 10^{-20}$ m^2/W – non-linear refractive index and A_{eff} – effective cross-section of the waveguide mode. The kernel $R(t)$ of the integral operator for non-linear response of the medium was taken from experiments referenced in [17]; it contains both electronic and vibrational (Raman) components. Expansion of the dispersion operator into the Taylor series in frequency was carried out to the highest term with $k_{max} = 3$. Although this may not be enough to model such a broad spectrum (from 1.2 μm to 1.78 μm) generated in the experiment, but the higher expansion terms were not given in the original experimental paper [8]. The second item in the right-hand side of Eq. (1) is responsible for a number of non-linear optical effects such as SPM, modulation instability (MI), stimulated Raman Scattering (SRS), four-wave mixing, self-steepening and shock formation [16].

The solution $A(z, t)$ of the Eq. (1) is found on a uniform analytical time grid covering – T_{max} to $+T_{max}$; since the employed algorithm of numerical integration uses fast Fourier transform (FFT) [16], the function $A(z, t)$ is assumed to be a $2T_{max}$-periodic function. This allows the radiation to go from one period into another, however we believe that it does not affect the calculation results noticeably. In order to check this we have done calculations with different periods (from 30 ps to ~ 4 ns for 3.5-W pump and from 30 ps to 240 ps for 4-W pump). The spectra generated in these calculations are virtually the same for different values of T_{max}. In order to simulate quantum noise we add one photon with random phase to each frequency mesh point.

3. Results and discussion

Given in Fig. 1 are the simulated spectra and time dependences of radiation intensity with the wavelength $\lambda_0 = 1486$ nm and the power $P_0 = 4$ W after passing different distances z in HNLF (with the dispersion coefficients $\beta_2 = -0.17$ ps^2/km, $\beta_3 = 0.0393$ ps^3/km measured in [8]). The initial phase of pump propagation through the fibre is marked by the development of modulation instability. For instance, at $z = 100$ m there are two definite peaks in the spectrum positioned symmetrically on each side of pump wavelength and separated from it by the frequency offset [16]

$$\Omega = \sqrt{\frac{2\gamma P_0}{|\beta_2|}} \approx 3.56\ \text{THz} \qquad (2)$$

#8055 - $15.00 USD Received 8 July 2005; revised 18 August 2005; accepted 22 August 2005

The peak in the long-wave spectral wing clearly visible at z = 100 m and z = 300 m is offset by 13 THz (104 nm) from the pump wavelength and resulted from SRS.

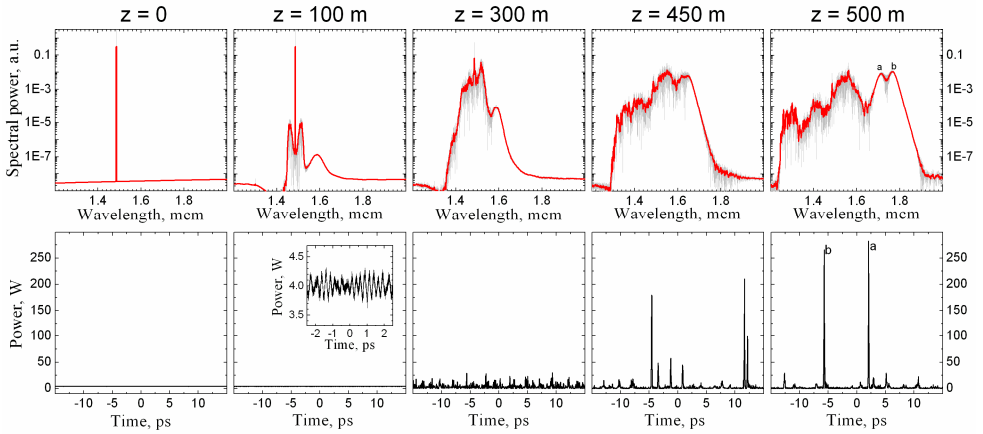

Fig. 1. Dynamics of SC generated by a CW pump radiation propagating through HNLF (simulation results). Upper graph row – spectra (smoothed spectra shown in red, unsmoothed ones, in grey), lower row – intensity vs. time after propagation over the distance z (corresponding values are given above the graphs). P_0 = 4 W, λ_0 = 1486 nm, β_2 = –0.17 ps^2/km, β_3 = 0.0393 ps^3/km.

Development of MI in time domain leads to oscillations with period of $T = 2\pi/\Omega \sim$ 0.28 ps. As the pump radiation propagates through the fibre oscillation amplitude grows and by z = 300 m the energy is travelling in the form of successive pulses. Some of these pulses have energy over soliton formation threshold, so optical solitons are produced and propagate through the fibre, experiencing self-frequency shift (SFS) due to SRS. At the same time some resonant energy transfer [18] occurs from solitons into normal dispersion region on the shorter-wavelength side of the pump wavelength, resulting in the growth of the total spectral width of continuum. In Fig. 1 at z = 500 m two optical solitons are visible, separated both in time and in spectrum domains. The latter circumstance comes from the fact that the soliton frequency down-shift is stochastic because of the noise present in the pump radiation. This is illustrated by a diagram in Fig. 2 where results of 50 numerical simulations are shown of 4-W CW pump propagation through 500-m-long HNLF. Each point corresponds to an optical soliton obtained in simulations. The higher the energy of a soliton is, the more (on the average) frequency shift it experiences; this is why the points in the diagram tend to group around a straight line. The full width of frequency distribution is about 5 THz which corresponds approximately to the spectrum width at z = 300 m (see Fig. 1). This can be explained by the fact that each soliton is formed at random location in the spectrum, so its carrier frequency at the exit from the fibre (at z = 500 m) is a sum of two random variables: $\nu_{sol}^{exit} = \nu_{sol}^{0} + \Delta\nu_{sol}(E_{sol})$ – initial soliton carrier frequency ν^0_{sol} (at the time of its formation) and the amount of soliton frequency shift $\Delta\nu < 0$ which depends on its energy E_{sol}.

Since the energy and soliton frequency shift are random parameters, the experimentally registered spectrum is broad and relatively smooth being a superposition of individual soliton spectra and accompanying non-soliton radiation. Analogous conclusions were made in previously published papers where CG was studied numerically with CW pump [15], as it was both numerically and experimentally with picosecond pumping pulses [19]. In order to compare numerical model predictions with experimental results we carried out a series of numerical simulations of CG with random noise in the pump radiation, upon which we averaged the collected spectra. The result of averaging over 50 simulations (with total grid width of 1.5 ns) is given in Fig. 3. When comparing it with experimental results reported in

#8055 - $15.00 USD Received 8 July 2005; revised 18 August 2005; accepted 22 August 2005

[8], an excellent quantitative and qualitative agreement is clearly seen. Thus, both in

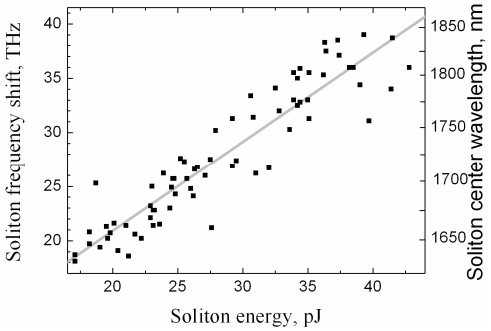

Fig. 2. Soliton frequency shift vs. soliton energy. Each point corresponds to a soliton obtained in simulations (P_0 = 4 W, λ_0 = 1486 nm, z = 500 m,β_2 = –0.17 ps^2/km, β_3 = 0.0393 ps^3/km).

simulations and in experiment a peak at the pump wavelength (λ_0 = 1.486 μm) is present as are a moderate dip at 1.45 μm, a peak at 1.42 μm, and a smooth steady decline in short-wave region down to 1.23 μm in simulations (and to 1.2 μm in experiment). Long-wavelength spectral wing is slightly higher than short-wavelength one, the feature being also present both in modelling and experiment. Discussing the differences between simulated and experimental spectra, first of all it is necessary to note a "fine structure" of the former – small oscillations of spectral power and a sharper (in comparison with experimental spectra) peak at pump wavelength. These discrepancies may have resulted from the fact that the averaging time in experiment is much longer than it is in simulations, thus leading to complete levelling of small oscillations and to certain smoothing of relatively large-scale peaks and dips of spectral power (averaging time in simulation was limited because of complexity of computer modelling). Another difference between the experimental results and model predictions, the mismatch of the position of short-wave spectral cut-off, may be caused by inaccurate modelling of fibre dispersion which is accounted for by only two expansion terms of $\beta(\omega)$ in Eq. (1). Near the edges of the studied spectral region the following terms of Taylor series may be significant, which is a potential reason of the mentioned discrepancy. However, within the 1.25 to 1.75-μm domain an excellent matching of experimental and numerical results has been achieved.

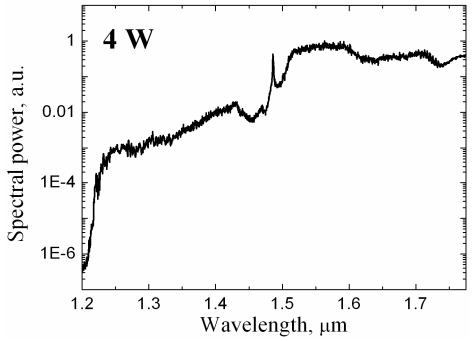

Fig. 3. Continuum spectra obtained by averaging of 50 results of numerical simulations (averaging time 1.5 ns). Parameters: CW pump with P_0 = 4 W, λ_0 = 1486 nm, 0.5-km-long HNLF with β_2 = –0.17 ps^2/km, β_3 = 0.0393 ps^3/km

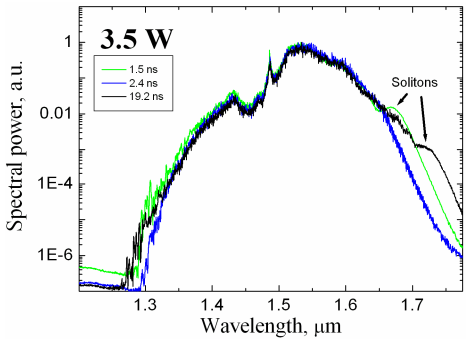

Fig. 4. Continuum spectra obtained by averaging results of numerical simulations with different averaging time (number of spectra averaged x 2T_{max}): 1.5, 2.4 and 19.2 ns for green, blue and black lines accordingly. Corresponding values of T_{max}: 15, 120 and 480 ps. Simulation parameters: CW pump with P_0 = 3.5 W, λ_0 = 1486 nm, 0.5-km-long HNLF with β_2 = –0.17 ps^2/km, β_3 = 0.0393 ps^3/km.

#8055 - $15.00 USD Received 8 July 2005; revised 18 August 2005; accepted 22 August 2005

As the pump power in the experiment [8] is reduced from 4 W down to 1.6 W, the spectral power in the wings of continuum also drops. At the edges of the examined spectral region (near 1.2 μm and 1.78 μm) the reduction of spectral power is about 20 dB while close to the pump wavelength it is only about 10 dB. Qualitatively, this behaviour can be explained in terms of the above-discussed formation of wide-band SC spectrum as superposition of individual soliton spectra. As the pump power is lowered the MI gain coefficient decreases linearly [16] and, therefore, length L_{MI}, at which MI develops and solitons form, increases. Correspondingly, length L-L_{MI} of the fibre stretch, in which propagation of solitons and SFS occurs, is reduced (here L=500 m is the fibre length). This leads, in turn, to the lower probability of formation of solitons with large frequency shift at the exit from the fibre. This may be one of the causes of larger observed drop in spectral power at the red wing of the spectrum when the pump power is lowered. Another cause of this may be the dependence of the soliton frequency shift upon soliton duration which, in its turn, depends on the repetition rate of pulses generated due to MI. Period between pulses is inversely proportional to a square root of the pump power [16], which also may lead to a lower probability of formation of solitons with large frequency shift when the pump power is reduced.

It is necessary to note that direct reproduction in simulation of experimentally obtained spectra for lower pump powers (P_0 = 1.6 W and 0.4 W) is further complicated because of growing demand on computer resources. Thus, when P_0 decreases from 4 W down to 1.6 W the experimentally observed spectral power near the spectral edges falls almost by two orders of magnitude (20 dB) – and consequently, the number of solitons generated in experiment in a unit time becomes 100 times smaller. In order to model a smooth spectrum one should preserve the number of solitons generated in simulations, but if the soliton formation probability is 100 times lower for low pump power, it is necessary to increase averaging time (number of simulations with random noise in pump) by two orders of magnitude.

Comparing the spectra obtained in the experiment [8] with pump powers P_0 = 4 W and P_0 = 1.6 W, one can see that the major difference between them consists in the magnitude of wings and a slightly narrower spectral width in the case of P_0 = 1.6 W. In this connexion one can expect that at intermediate levels of P_0 (between 1.6 and 4 W) the spectral shape will remain unchanged. On the basis of this assumption it is possible to compare predictions of numerical model and experimentally obtained dependence of SC spectrum on pump power, setting P_0 only a slightly lower than 4 W (for example, 3.5 W). This should allow us to reduce appreciably the computational load since the spectral wings magnitude, number of solitons generated in a unit time and, correspondingly, the necessary amount of sampling would be only moderately different from the case of P_0 = 4 W, and not by a factor of 100.

Figure 4 shows the numerical SC spectra taken by averaging the results of simulations with different averaging time (corresponding values are given in the graph legend). Contrary to what can be expected from the analysis of experimental results [8], spectra simulated with different pump powers not only demonstrate various wing magnitude, but also have different width and shape. In spite of the fact that isolated solitons are visible in the averaged spectra shown in Fig. 4, insufficient sampling volume is unlikely the cause of such a considerable disagreement with the experiment. Indeed, when the averaging time is increased more than by an order of magnitude (from 1.5 ns to 19.2 ns, see Fig. 4) the spectrum does not become significantly wider.

In order to find out the mechanism of the unexpectedly strong dependence of the spectrum width of the modelled SC upon the pump power, let's once more consider Fig. 1 where the dynamics of radiation travel along the fibre is given. From Fig. 1 it can be seen that the process of MI development culminates in soliton formation within the interval between 300 and 450 m. Because the development of MI is the longest phase (see Fig. 1) it may be expected that the fibre length in which solitons are generated is inversely proportional to the MI gain coefficient and, consequently [16], to the pump power. Taking for the sake of estimation L_{MI} = 400 m at P_0 = 4 W, we will have L_{MI} = 457 m at P_0 = 3.5 W. Accordingly,

#8055 - $15.00 USD Received 8 July 2005; revised 18 August 2005; accepted 22 August 2005

the length of fibre stretch L-L_{MI} where self frequency shift of solitons develops is now reduced from 100 m to 43 m, that is by a factor of 2.3 when the pump power was reduced by only 12.5% (from 4 to 3.5 W). It is this dramatic shortening of the self frequency shift stage for solitons that leads to the observed in our calculations sharp reduction of the spectrum width. Hence, the power level P_0 = 4 W is, in the framework of this model and at the used parameters, only slightly above the threshold. This fact, together with inaccuracy of dispersion terms, may also account for the above-mentioned mismatch between the calculated and the experimental spectra around 1.2 μm at P_0 = 4 W.

The absence of power threshold in the experiment around P_0 = 4 W may be due to the presence in the pump radiation of intensity fluctuations, which are not taken into consideration in our model. Fluctuations of intensity may lead to a significant shortening of the soliton generation phase because in this case the formation of a pulse train, from which solitons are generated, is triggered by amplification of a noise, which is initially much higher than the quantum one.

Conclusions

The developed method of description of CG with CW pump on the basis of quantum noise model and averaging over large number of spectra demonstrates for the first time a remarkable qualitative and quantitative agreement with experiment [8] at maximum pump power level of 4 W. At lower pump levels, for adequate description of experimental results the present numerical model also has to take into account amplitude noise in the pump radiation. It is expected that the calculations will be complicated by a steep growth of computational complexity. On the basis of the generated simulation results we also discussed a qualitative explanation of broad-band and relatively smooth continuum spectrum generation.

The proposed method of simulation of spectrum broadening of CW radiation propagating through HNLF may be used, in particular, for modelling and optimisation of broad-band Raman amplifiers, in which the spectral broadening of pump lines is induced by MI [20].

Acknowledgments

This work was supported by the INTAS, project No. 03-51-5288.

#8055 - $15.00 USD Received 8 July 2005; revised 18 August 2005; accepted 22 August 2005